

Gao et al., <http://www.jgp.org/cgi/content/full/jgp.201311112/DC1>

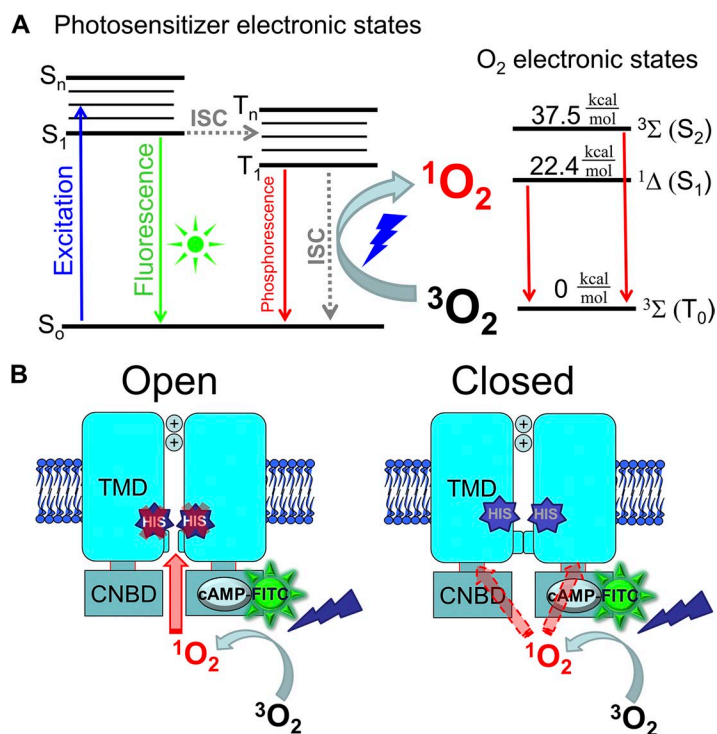


Figure S1. 1O_2 production through photosensitization process and the working model for 1O_2 modification of HCN channels. (A) ISC refers to intersystem crossing between singlet (S) and triplet (T) spin multiplicity states (Ogilby, 2010. *Chem. Soc. Rev.* 39:3181–3209). The longer lifetime of Tn states is essential for the production of 1O_2 . (B) Working model for the modification of HCN channel by photochemically generated 1O_2 .

DNA and protein sequences of mHCN2-EGFP construct

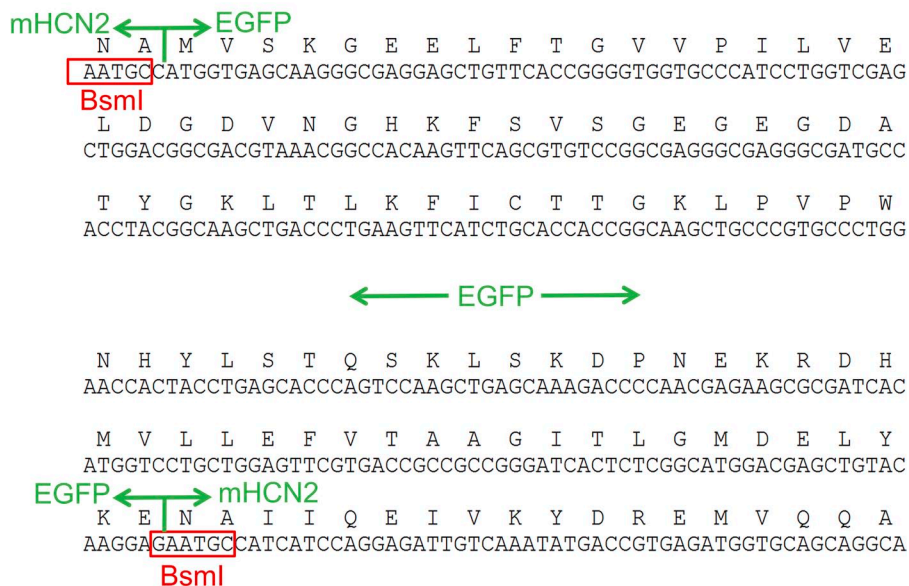


Figure S2. Construction of the mHCN2-EGFP fusion channel.

DNA and protein sequences of mHCN2-SOG construct

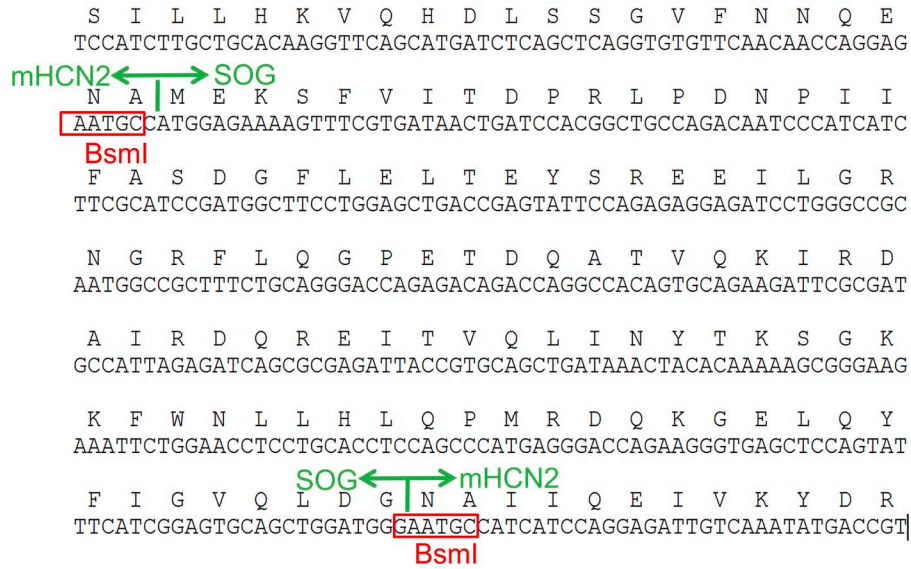


Figure S3. Construction of the mHCN2-SOG fusion channel.

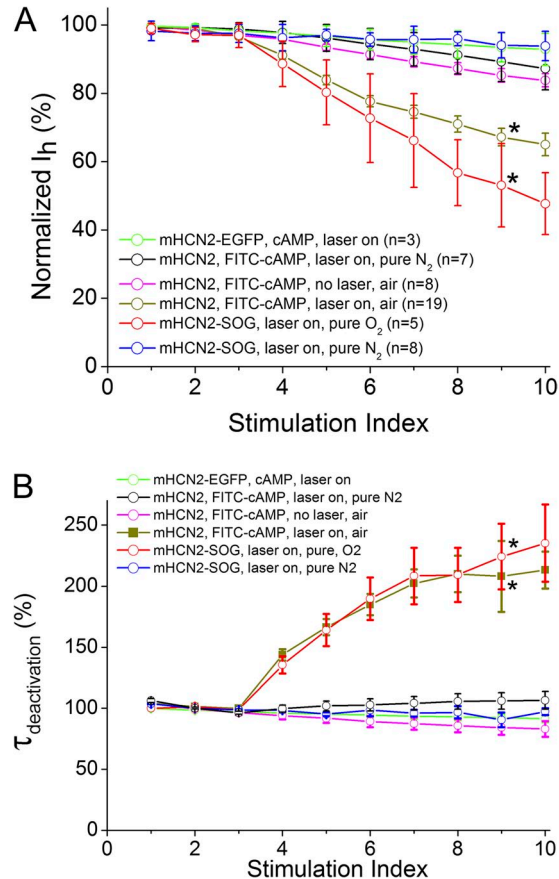


Figure S4. Decrease of I_h amplitude under different conditions. (A) Amplitude of I_h current was normalized to the maximal current ($I_h + I_{inst}$). The concentration of cAMP or FITC-cAMP was 0.5 μ M. *, $P < 0.05$ (one-way ANOVA followed by Tukey's post-hoc test). (B) Normalized time constant for channel deactivation. *, $P < 0.05$.

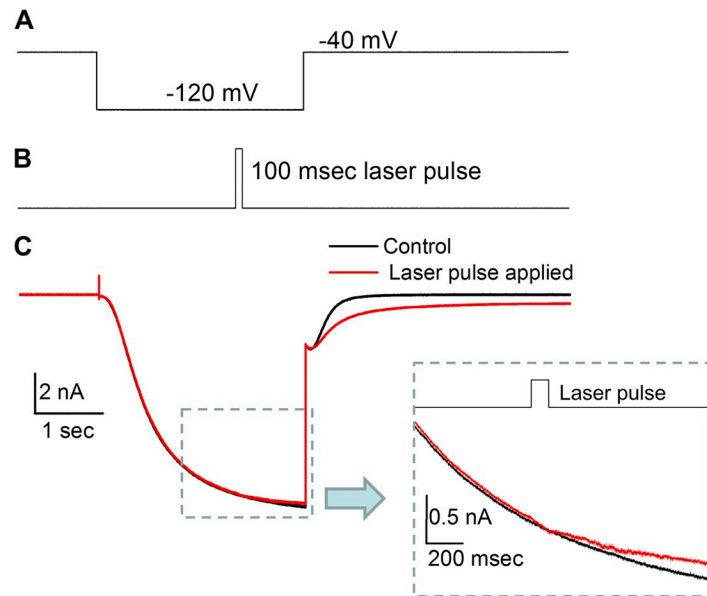


Figure S5. Current traces at the moment when the laser pulse was delivered. (A) Voltage protocol for channel activation. (B) Timing of the 100-ms laser pulse. (C) Overlay of the current traces before (black) and with laser pulse applied (red). A close-up view of the moment when the laser pulse was applied is shown in the bottom-right corner.

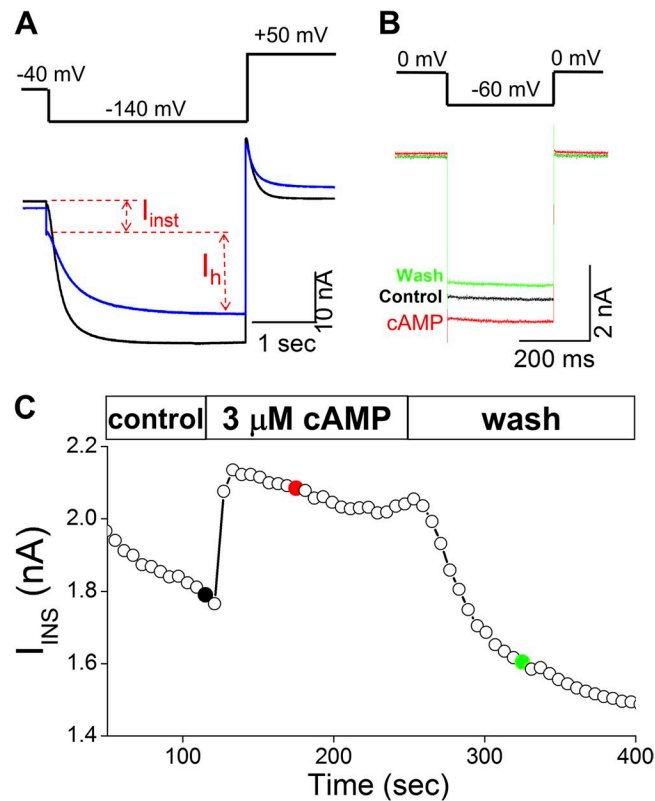


Figure S6. cAMP enhances photochemically generated I_{inst} . (A) Current traces in response to a hyperpolarizing voltage step before (black) and after (blue) laser pulses. The components of I_{inst} and I_h have been marked for the current trace after laser pulses (blue). (B) The I_{inst} recorded from the patch shown in A. Three traces were recorded before (black), during (red), and after cAMP application (green). To prevent the activation of I_h , a voltage step to -60 mV was used to record I_{inst} . (C) Time course of I_{inst} amplitude before, during, and after cAMP application. Timing of the three current traces shown in B is indicated. This experiment was repeated five times. The corresponding negative control membrane patches from uninjected oocytes exposed to cAMP are shown in Fig. S7.

Currents recorded from uninjected oocytes.

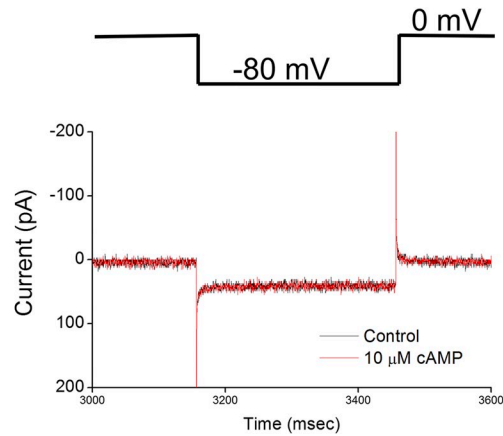


Figure S7. Negative control of cAMP-enhancing I_{inst} : membrane patches from uninjected oocytes. Membrane patches were pulled from the surface of uninjected oocytes. Ionic current was driven by a hyperpolarizing voltage step to -80 mV. After six episodes were collected as the control, $10 \mu\text{M}$ cAMP, 20 times higher than the typical concentration used in this study ($0.5 \mu\text{M}$), was applied to the bath solution. No obvious increase in the baseline (leak) current was observed. This experiment was repeated four times.

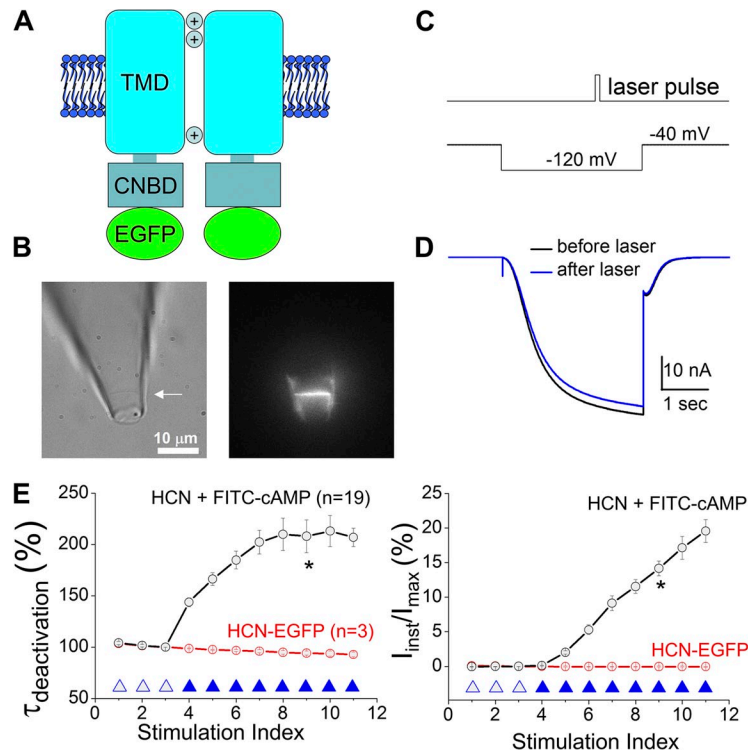


Figure S8. Laser treatments of membrane patches expressing HCN-EGFP did not generate I_{inst} . (A) The mHCN2-EGFP fusion channel. (B) Bright field and fluorescence images of the membrane patch expressing mHCN2-EGFP channels. Arrow indicates the position of the membrane patch. (C) Timing of the laser pulse and the voltage protocol used for channel activation. Laser pulses were given during the channel activation, the same as in Fig. 2 in the main text. (D) Current traces before (black; no. 3 in E) and after (blue; no. 7 in E) laser treatment. (E) Average $\tau_{deactivation}$ (left) or percentage of I_{inst}/I_{max} (right) versus episode number. *, $P < 0.05$.

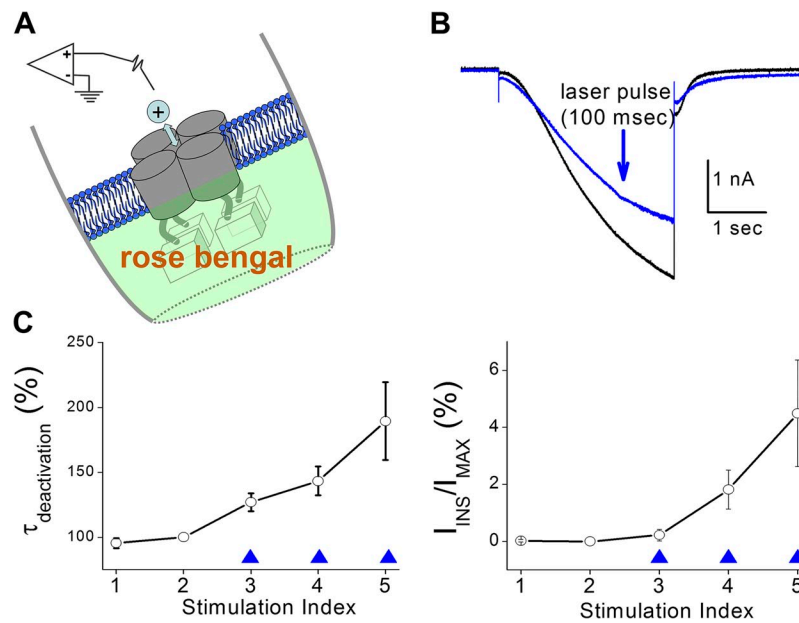


Figure S9. Rose bengal was used as the photosensitizer in the photodynamic transformation of the mHCN2 channel. (A) 100 nM rose bengal was applied to the intracellular side of the membrane patch. (B) 100-ms laser pulses were delivered during the 3-s hyperpolarizing voltage step. Black, control; blue, current trace after laser treatment. (C) Averaged $\tau_{\text{deactivation}}$ (left) or percentage of I_{inst} (right) versus episode number. Laser pulses were delivered from the third episode ($n = 3$).

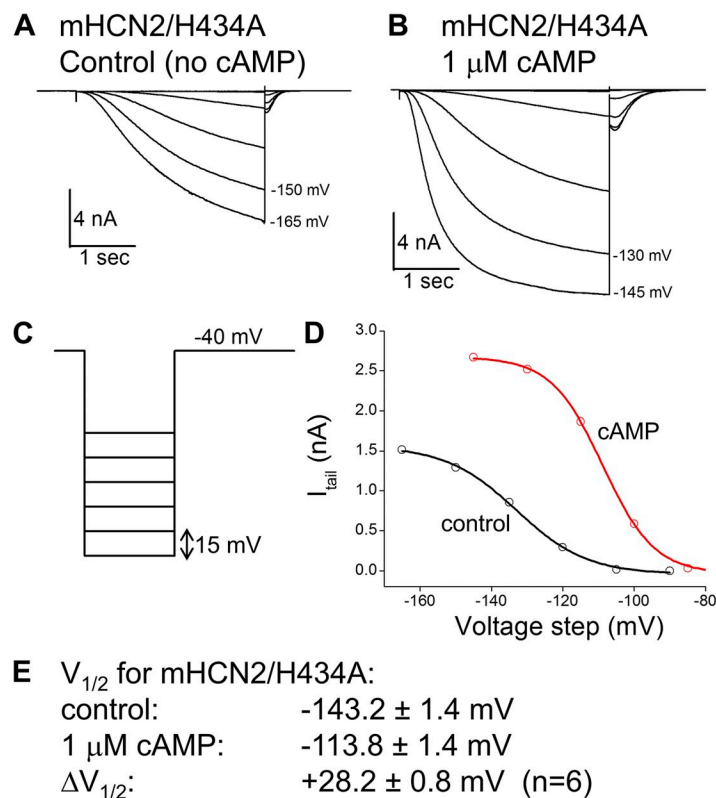


Figure S10. cAMP enhances the gating of the mHCN2/H434A mutant channel. (A) Current traces of mHCN2/H434A in response to a series of voltage steps in -15-mV intervals (shown in C). No cAMP was added. (B) Current traces of mHCN2/H434A in the presence of $1\ \mu\text{M}$ cAMP. (C) Voltage protocol used for collecting the I-V curve. (D) I-V curves of the current traces shown in A and B. Tail currents were measured at a holding potential of -40 mV. (E) Summarized $V_{1/2}$ results.

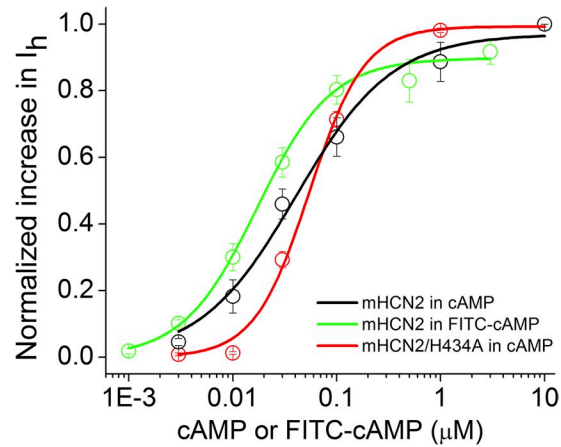


Figure S11. Dose–response curves showing FITC-cAMP or cAMP to enhance the I_h current. HCN channels were activated by a hyperpolarizing voltage step to -130 mV for the WT mHCN2 channel or to -140 mV for the mHCN2/H434A mutant channel. Different concentrations of FITC-cAMP or cAMP were sequentially added to the bath solution. The increases in I_h amplitude for each patch were normalized to the maximal value obtained with 10 μ M cAMP. For FITC-cAMP, the EC_{50} value is 0.017 ± 0.002 μ M (WT mHCN2 channel). For cAMP, the EC_{50} values are 0.041 ± 0.008 μ M (WT mHCN2 channel) and 0.054 ± 0.004 μ M (mHCN2/H434A mutant channel).

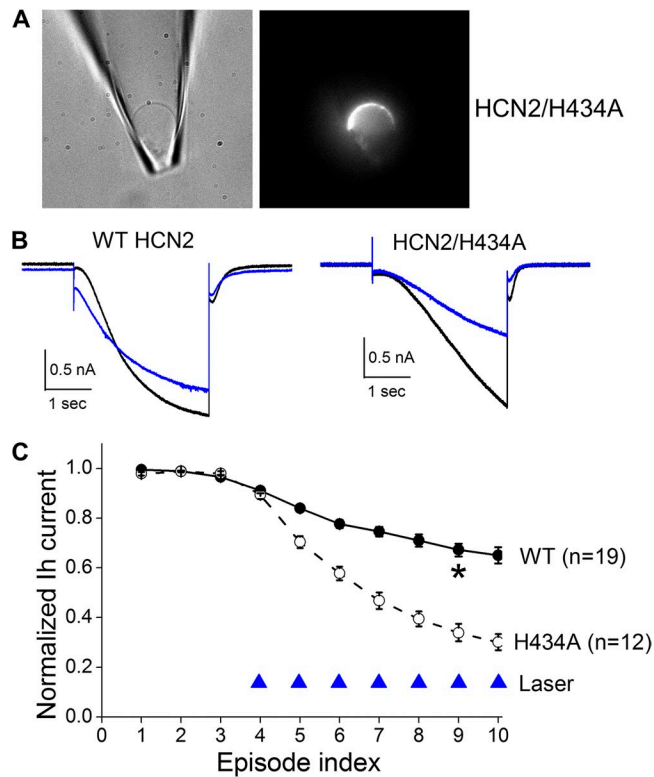


Figure S12. Decreases of the I_h current amplitude in WT mHCN2 and mHCN2/H434A mutant channels. (A) Bright field (left) and fluorescence image (right) of a membrane patch expressing mHCN2/H434A mutant channel. 0.5 μ M FITC-cAMP was added to the bath solution. (B) Current traces before (black; no. 3 in C) and after (blue; no. 8 in C) laser pulses. Membrane patch was held at -40 mV, and a hyperpolarizing voltage step to -140 mV was used to activate the channel. (C) Normalized I_h current amplitude versus episode number. Laser pulses were applied from number 4. *, $P < 0.05$ (one-way ANOVA followed by Tukey's post-hoc test).

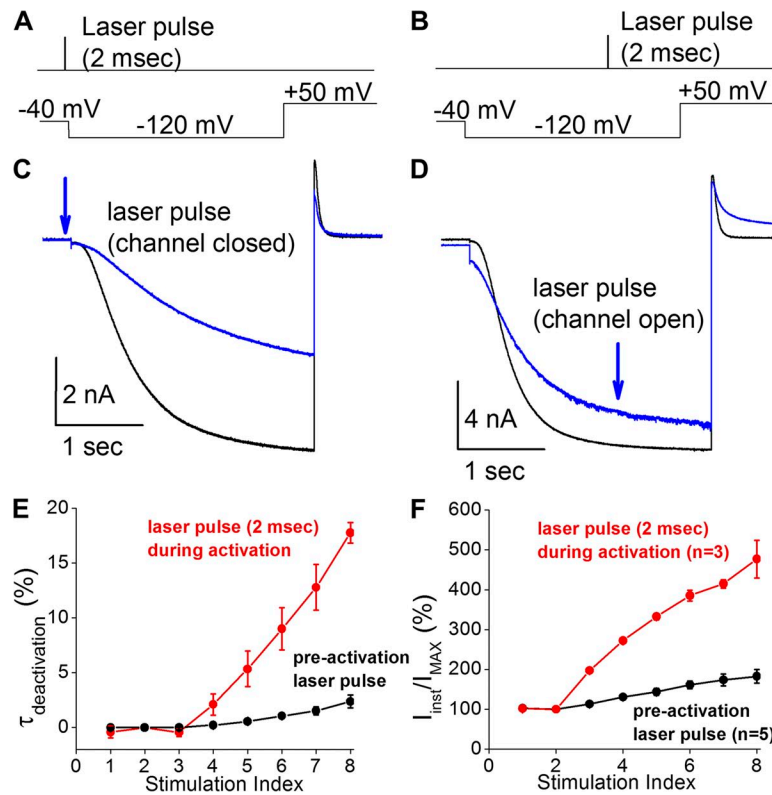


Figure S13. Photodynamic transformation of the HCN channel by short laser pulses (2 ms). $^1\text{O}_2$ is known to have a short lifetime (10^{-6} sec), but most previous studies used long light irradiation—from seconds to minutes—to produce observable effects. Here we show that brief laser pulses (2 ms) were able to transform the HCN channel, still in a state-dependent manner. The laser intensity ($\sim 14 \text{ W/cm}^2$) was ~ 40 times higher than typically used in this study. The same concentration of FITC-cAMP ($0.5 \mu\text{M}$) was used. Solutions were degassed and then purged with pure oxygen. (A) Timing of the 2-ms laser pulse and the hyperpolarizing voltage step. Laser pulses were delivered before the voltage step when most channels stayed in the closed state. (B) Laser pulses were delivered during the voltage step when most channels were in the open state. (C and D) Current traces before (black) and after laser treatment (blue). (E) Average time constant of deactivation versus episode number. (F) Percentage of I_{inst} versus episode number.